2022 IEEE Energy Conversion Congress and Exposition (ECCE) | 978-1-7281-9387-8/22/$31.00 ©2022 IEEE | DOI: 10.1109/ECCE50734.2022.9947859

Optimizing Sensor Count and Placement to Detect Bond Wire Lift-offs and Surface Defects in High-Power IGBT Modules using Low-Cost Piezo-electric Resonators

Tohfa Haque
Dept. of computer science electrical engineering
University of Missouri, Kansas City
Kansas City, USA
thpcd@umsystem.edu

Abu Hanif
Dept. of computer science electrical engineering
University of Missouri, Kansas City
Kansas City, USA
abu.hanif@umkc.edu

Faisal Khan
National Renewable Energy Laboratory
Golden, USA
faisal.khan@nrel.gov

Abstract— **This manuscript presents the most recent results and findings to identify bond wire lift-offs and surface defects in high-power isolated gate bipolar junction transistor (IGBT) modules. The authors of this manuscript formerly proposed a low-cost, piezoelectric resonator-based measurement unit to detect bond wire related degradation in larger IGBT modules. Since high-power IGBT modules are expensive, it was apparent that evaluating our proposed method by inducing controlled damage to fresh (new) IGBTs may not be cost-effective especially when multiple sets of data need to be captured by inducing damage to different levels. In order to overcome this limitation, IGBT bond wires have been mimicked using a 3D printed enclosure, a PCB, and copper wires with dimensions very closely resembling a real IGBT. Using this method, multiple test devices can be built at the cost of a real IGBT, and the proposed technique could be fine-tuned without damaging expensive, real IGBTs. Our recent findings can be used to determine real IGBT degradation and bond wire lift-offs using only two sensors, as opposed to six transducers used in the first iteration of the setup. In addition to optimizing the sensor count, we have also identified the best possible locations of these sensors by attempting multiple placements inside the IGBT casing.**

Keywords— Imitation IGBT, piezoelectric transducers, condition monitoring, reliability, ultrasound.

I. Introduction

The role of power electronic converters is crucial in a wide range of applications such as power generation, industrial power systems, locomotives, renewable energy integration, motor drives, and so on. Reliability is one of the major concerns for these high-power and high-voltage converters. Any downtime due to converter failure is not expected in applications such as transportation, smart grids, industrial drives, and in many other critical applications. For example, converters with relatively low reliability increase the maintenance cost and decrease the system availability. An estimated 34% of power electronics application failures are related to power semiconductor devices [1-2]. Therefore, an online condition monitoring method is necessary to prevent unwanted and premature failures.

Environmental stress factors such as ambient temperature, vibration, humidity, and cyclic thermal stress contribute to the degraded performance of power semiconductor devices. Conventional methods can predict the reliability of components such as mean time to failure (MTTF). However, MTTF predicts expected lifespan, but cannot be used to predict unusual circumstances or continuous overstress and premature degradation. These stresses collectively propagate to package-related failures and eventually causes circuit-level malfunctions. In spite of the fact that MTTF must be overly conservative, it still cannot adequately predict the failures that plague power systems. When IGBTs fail before their MTTF due to stress, this brings down the system and causes economic, safety, and environmental problems.

The internal temperature of a power converter can swing up to 80℃, which significantly affects the health of the solid-state switches. Due to these stresses, voids are formed at the bond pad resulting in elevated junction temperature. For IGBTs, two kinds of failures exist i) chip-related (or intrinsic) failure and ii) package-related (or extrinsic) failure. Chip-related failures mostly occur due to electrical overstress such as high-voltage and high-current through the devices. Package-related failures are mostly related to thermo-mechanical overstress. This overstress is caused by any mismatch in the coefficient of thermal expansion (CTE) between the silicon die and copper substrate. This mechanism eventually results in bond wire (BW) lift-offs or detachments [3-5].

Many condition monitoring methods have been proposed in the past, and all of them have their strengths and limitations. The novelty of this research work is that low-cost sensors can be placed inside existing IGBT modules, and the results are independent of devices' operating points such as junction temperature or voltage/current level. Since the detection method is acoustic, results are not strongly correlated to incident electric and magnetic fields. The co-author formerly proposed a spread spectrum time domain reflectometry (SSTDR) based scheme to detect IGBT bond wire lift-off [6-7] and the state of health (SOH) of other power components in a circuit. However,

• This project is funded by National Science Foundation (NSF) grant no.1947410.

Authorized licensed use limited to: University of Missouri Libraries. Downloaded on June 03,2023 at 08:53:52 UTC from IEEE Xplore. Restrictions apply.

SSTDR-based techniques suffer from several limitations such as the hardware being limited by 48MHz of the center frequency. In contrast, the proposed technique could bring useful SOH information using a very low-cost implementation. In addition, this proposed method has several advantages over the existing V_{CE} measurement-based method traditionally used to determine IGBT aging. Firstly, the V_{CE} measurement-based method is unable to specify the number of bond wire lift-offs and their corresponding locations. Therefore, it is unsuitable to identify whether the degradation is due to the operational condition or any manufacturing process variation. In contrast, the ultrasound-based method will be able to identify the location and number of detached bond wires. This information is quite meaningful. According to the existing reliability research, any major change in V_{CE} occurs right before the device completely fails, and it is not sensitive enough to predict gradual degradation. In addition, aging measurement using V_{CE} greatly depends on the load current. Therefore, gradual degradation cannot be accurately determined using the V_{CE} method. In contrast, our proposed method is independent of I_{CE}, and the technique can conduct direct measurement of the actual damage inside the IGBT module [8].

Acoustic waves can be effectively used to detect the health of power semiconductor devices especially the ones with bond wires. One of the most commonly used ultrasound-based methods is Confocal Scanning Acoustic Microscopy (CSAM), which is a non-destructive technique. It measures the mismatch of acoustic impedances to determine the state of health of IGBTs. To measure IGBT health, it module/device needs to be submerged in a couplant. However, due to the size of the test setup and the need for another fluid medium, this technique cannot be implemented for live condition motoring [9]. In addition, the existing solutions are not sufficiently compact to place inside a commercially available IGBT module. In contrast, Electromagnetic Acoustic Transducers (EMAT) operate without a fluid medium, and with the use of coils and magnets, it can construct complex wave patterns. The coil must be excited with a high current, and the transducer is able to generate only low-frequency waves. Therefore, EMAT accuracy is low, and it decreases with the distance between the IGBT bond wire and transducer [10-11]. On the other hand, our proposed method has several advantages over the existing methods, described as follows:

1. It uses low-cost piezoelectric ultrasound resonators to detect any bond wire detachments inside the IGBT module.
2. An attractive feature of this method is that it can replace the complex calculation or complicated arrangement to monitor the health of IGBT.
3. This proposed method can provide an instant and continuous output which can be compared to the healthy condition result of IGBT.
4. The proposed method is not temperature and current dependent and can detect the degradation of IGBT using the sampled data.

II. Proposed Method

The reflection property of ultrasound waves can be utilized to detect any bond wire detachments induced by package-related failures inside the power-switching devices. The proposed testing method is non-destructive evaluation (NDE) in nature, and low-cost ultrasound piezoelectric transducers have been used inside the IGBT enclosure to detect bond wire lift-offs. This approach has many advantages such as the ability to integrate with the gate driver circuit, and the accuracy of this technique can be controlled by changing the number, location,

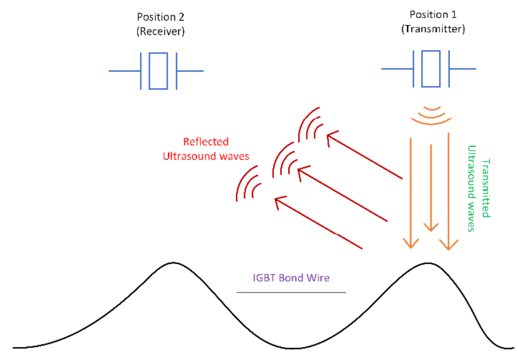

Figure 1. Sensor positioning, wave propagation and the reflection path

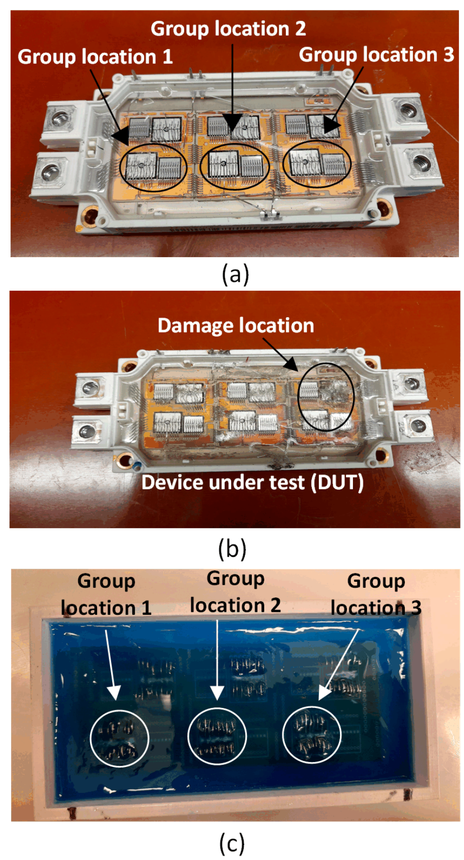

Figure 2. Inside view of (a) healthy (b) damaged and (c) imitation IGBT.

Authorized licensed use limited to: University of Missouri Libraries. Downloaded on June 03,2023 at 08:53:52 UTC from IEEE Xplore. Restrictions apply.

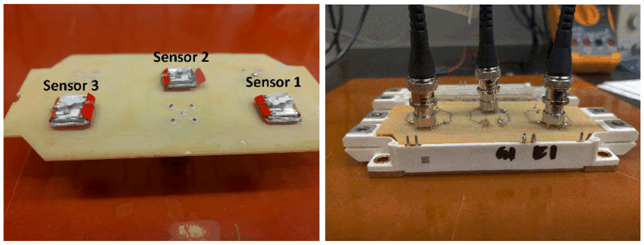

(a) (b)

Figure 3. Test 1 (three 50MHz sensors, real IGBT): (a) Three 50MHz piezoelectric transducers has been placed on the PCB and (b) the completed prototype showing the BNC connectors with real IGBT.

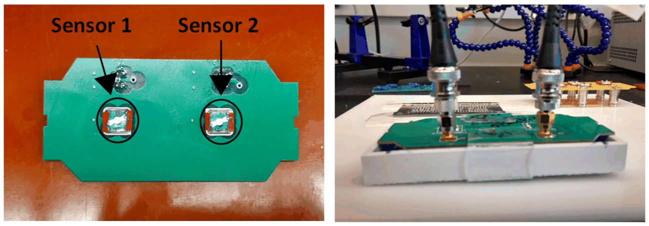

(a) (b)

Figure 4. Test 2 (two 20MHz sensors, imitation IGBT) (a) Two 20MHz piezoelectric transducers has been placed on the PCB and (b) The completed prototype showing the BNC connectors with SMA to BNC in the PCB with imitation IGBT.

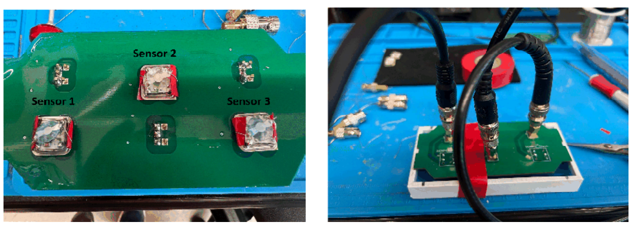

(a) (b)

Figure 5. Test 3 (three 20MHz sensors, imitation IGBT) (a) Three 20MHz piezoelectric transducers has been placed on the PCB and (b) the completed prototype showing the BNC connectors with imitation IGBT.

and frequency of the sensors. To execute this experiment, 20MHz and 50MHz piezoelectric transducers have been used with two different test setups. During each test, two transducers work in conjunction – one transducer acts as the transmitter and the other as the receiver. In the past, the co-author proposed a 6-resonator solution with one working as a transmitter and the remaining five as the receivers using a 25MHz ultrasound signal. In order to optimize the number of sensors and find the best resonator placement, authors have attempted different combinations of location and frequency. Once optimized, the proposed method is quick and can provide exact number of bond wire detachments. At first, a baseline dataset is created by applying the technique to a healthy IGBT. Then another set of reflection data are obtained from the receiver sensor/resonator for the aged IGBT with damaged/detached bond-wire. The magnitude and the shape of the reflected wave will depend on several factors such as: (1) the location of the detached bond wire(s), (2) number of detached bond wires, (3) resonator frequency, and (4) transmitter output magnitude.

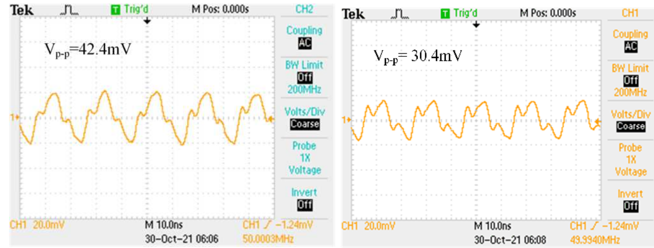

(a) (b)

Figure 6. Time-domain data for test 1 from sensor 2 for (a) healthy and (b) damaged IGBT with a three-sensors setup of 50MHz.

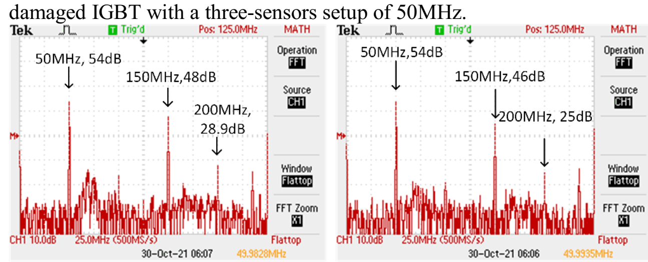

(a) (b)

Figure 7. Frequency domain data for test 1 from sensor 2 for (a) healthy and (b) damaged IGBT with a three-sensors setup of 50MHz.

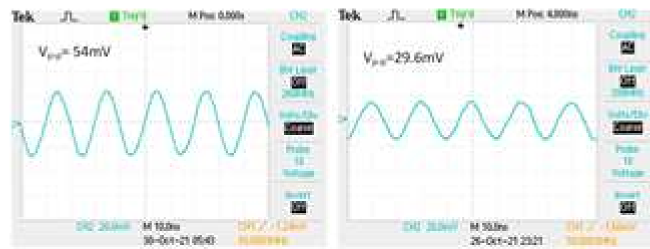

(a) (b)

Figure 8. Time-domain data for test 1 from sensor 3 for (a) healthy and (b) damaged IGBT with three-sensor setup of 50MHz.

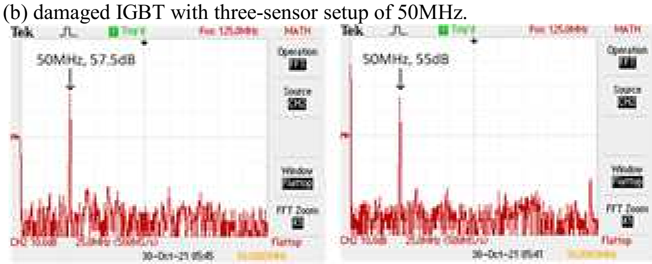

(a) (b)

Figure 9. Frequency domain data for test 1 from sensor 3 for (a) healthy and (b)damaged IGBT with three-sensors setup of 50MHz

III. EXPERIMENTAL SETUP AND RESULTS

Ultrasound waves can be transmitted and received using ultrasound resonators. The reflection coefficient carries the information of the impedance mismatch between two mediums since the ultrasound wave is reflected from the medium interface. Let us assume the acoustic impedance of one medium is Z_1, and the impedance of the second medium is Z_2. The reflection coefficient (R) can be calculated from the equation shown below [12]:

$$R = \left(\frac{Z_2 - Z_1}{Z_2 + Z_1}\right)^2 \quad (1)$$

The experiment was partially conducted using FF450R12ME4, a dual pack IGBT module rated at 1200V and 900A, and the rest of the experiment was conducted using an imitation IGBT. There is a silicone gel layer covering the chip

Authorized licensed use limited to: University of Missouri Libraries. Downloaded on June 03,2023 at 08:53:52 UTC from IEEE Xplore. Restrictions apply.

dies in the actual dual-pack IGBT, which protects the wire bonds against environmental stresses such as humidity, ambient temperature, and moisture. The imitation IGBT has a similar silicone gel layer for data integrity. Once triggered, the ultrasound signal propagates from the transmitter through half of the silicone gel thickness, which has an acoustic impedance of Z_2. During reflection, the wave propagates through the bond wires (acoustic impedance is Z_1), and then reaches the receiver piezoelectric resonator [13]. Before it reaches the receiver, the signal propagates twice halfway through the silicone gel, and the corresponding propagation paths and wave reflections are shown in Figure 1. The reflection coefficient (R) carries meaningful information such as surface damage, number and location of detached bond wire(s) and so on. In order to analyze the effect of different types of damages without destroying a real IGBT, we have constructed an imitation IGBT with bond wires, which mimics the geometry of a real IGBT bond wire assembly as shown in Figure 2(c). Figure 2(a) represents a dual-pack IGBT module in healthy condition and Figure 2(b) illustrates the inside view of a damaged IGBT. This imitation IGBT is made from single-stranded solid wires, a PCB, and a 3D printed enclosure, and this arrangement can be inexpensively fabricated and can be used to generate realistic data without inducing damage to a real IGBT. To create a comparative analysis, three test arrangements have been made. Test 1: Three 50 MHz sensors have been used with a real IGBT, Test 2: two 20 MHz sensors have been used with an imitation IGBT, and Test 3: three 20 MHz sensors have been used with another imitation IGBT. All experimental data have been captured using a Tektronix TPS2024B oscilloscope.

Three different PCBs have been designed to execute the experiment, and the ultrasound transducers have been placed on each PCB in different combinations of location and frequency. Figure 3(a) shows three 50 MHz piezoelectric resonators that have been placed on the PCB, and figure 3(b) shows the experimental setup. Figure 4(a) shows the bottom view of the sensor PCB and the location where two 20MHz sensors have been used and Figure 4(b) demonstrates the corresponding test setup. Figure 5 shows the test setup for the three-sensor 20 MHz system using the imitation IGBT.

Figure 6 illustrates the time domain data of sensor 2 for the three-sensor setup (Test 1: real IGBT, 50 MHz) of the healthy and damaged IGBT, and Figure 7 illustrates the same in the frequency domain. Figure 8 and Figure 9 demonstrate the time-domain and frequency-domain data obtained from sensor 3 of the three-sensor setup (Test 1: real IGBT, 50 MHz). Figure 6(a), Figure 7(a), Figure 8(a), and Figure 9(a) represent the corresponding healthy data, and Figure 6(b), Figure 7(b), Figure 8(b), and Figure 9(b) shows the reflection data for the damaged ones. For example, (in Figure 6(a) and Figure 7(a)) in the time domain output obtained from sensor 2 for a healthy IGBT, the peak-to-peak voltage (V_{P-P}) was 42.4mV, whereas it was V_{P-P}=30.4 mV for an IGBT with damaged bond wires. Similarly, sensor 3 produces a 24.4mV difference (shown in Figure 7) in $V_{P-P,}$ indicating the induced damage inside the IGBT. In addition, the differences in time domain data are also reflected in frequency domain output. We have seen changes in both fundamental and its harmonic components, and these data points are summarized in Table I. However, this initial study is only

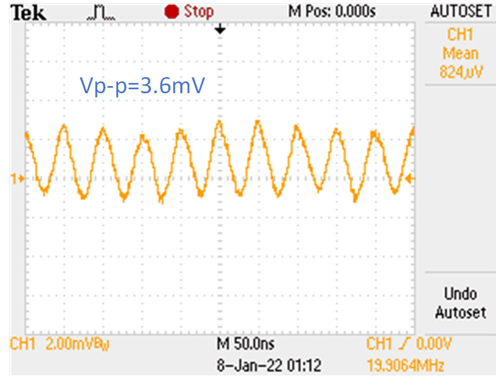

(a) Initial condition

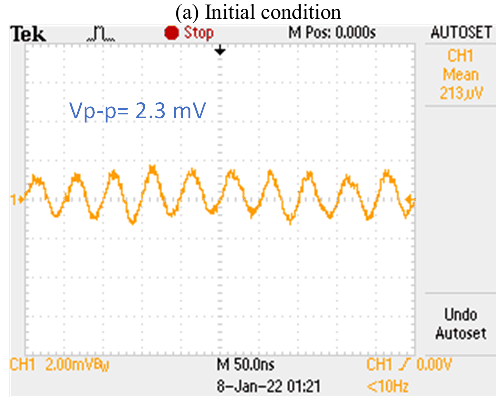

(b) Single detached bond wire

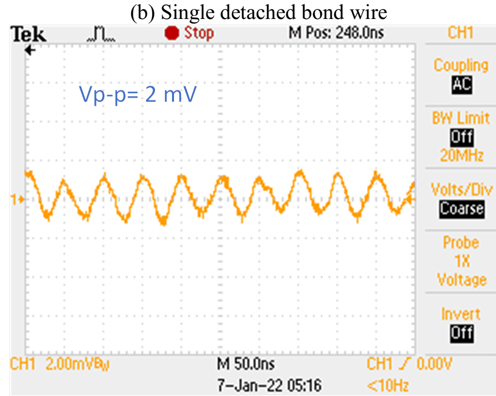

(c) Two detached bond-wires

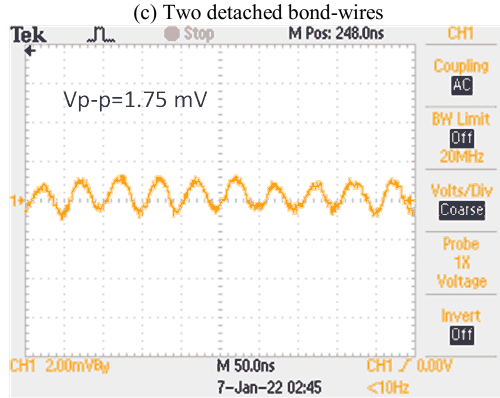

(d) Three detached bond-wires

Figure 10. Time domain data for test 2 of receiver sensor for 20MHz two sensors set up in different health status with imitation IGBT.

Authorized licensed use limited to: University of Missouri Libraries. Downloaded on June 03,2023 at 08:53:52 UTC from IEEE Xplore. Restrictions apply.

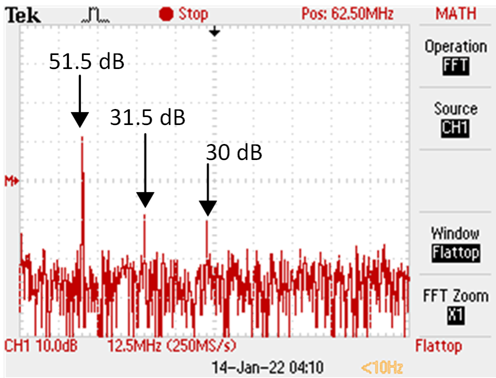

(a) Initial condition

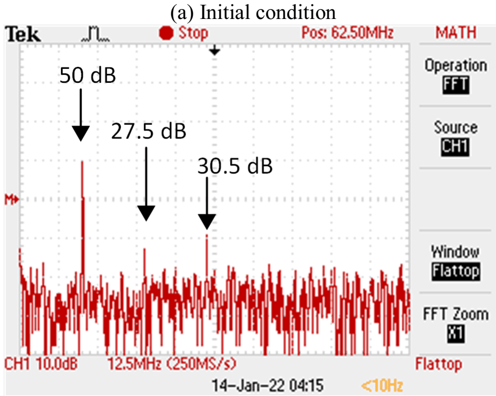

(b) Single detached bond-wire

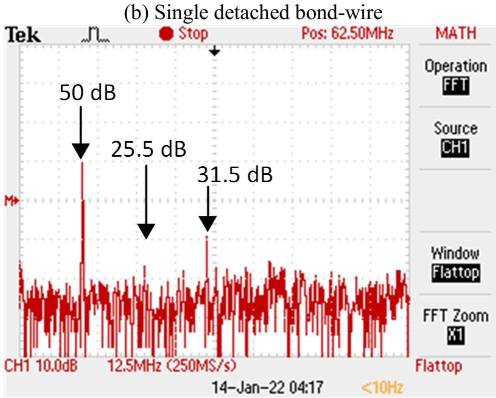

(c) Two detached bond-wires

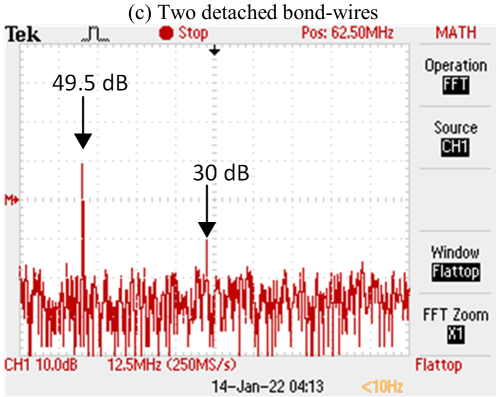

(d) Three detached bond-wires.

Figure 11. Frequency domain data of test 2 of receiver sensors for 20MHz two sensors set up with imitation IGBT.

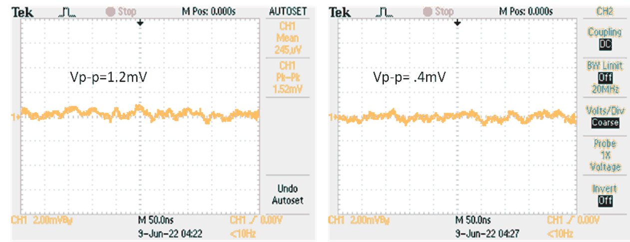

(a) (b)

Figure 12. Time-domain data for test 3 from sensor 2 for (a) healthy and (b) single wire detached IGBT with a three-sensors setup of 20MHz (ΔV_{P-P}=0.8mV).

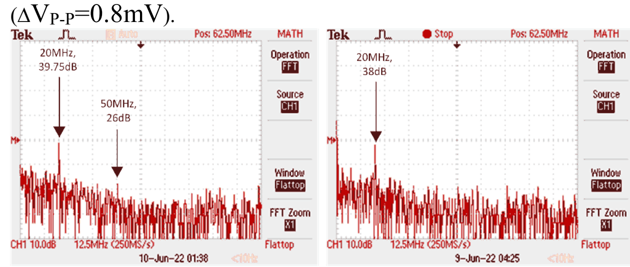

(a) (b)

Figure 13. Frequency domain data for test 3 from sensor 2 for (a) healthy and (b) single wire detached IGBT with a three-sensor setup of 20MHz (ΔV_{P-P}=0.4mV).

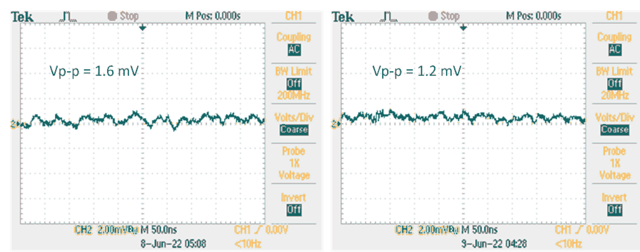

(a) (b)

Figure 14. Time-domain data for test 3 from sensor 3 for (a) healthy and (b) b) single wire detached IGBT with a three-sensors setup of 20MHz (ΔV_{P-P}=0.8mV).

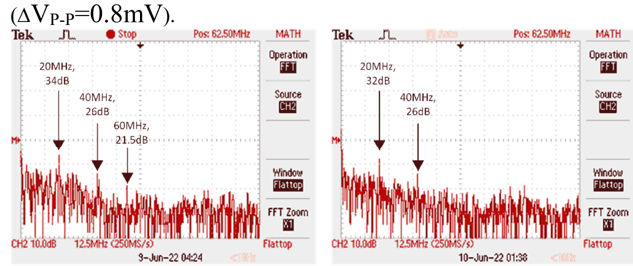

(a) (b)

Figure 15. Frequency domain data for test 3 from sensor 3 for (a) healthy and (b) single wire detached IGBT with a three-sensor setup of 20MHz.

confined to detecting any degradation at a given location of the IGBT.

Figure 10 illustrates the time domain output for different health conditions of the imitation IGBT executing with a two-sensors system (Test 2: two 20MHz sensor, imitation IGBT) and a 20MHz ultrasound wave has been used to produce this experimental data. For the undamaged (initial) condition, the peak-to-peak output voltage (V_{p-p}) is 3.6mV. This output drops to V_{p-p}= 2.3mV once a single bond wire is detached. During two detached bond wires, V_{p-p} becomes 2mV (Fig. 10(c)), and the output is 1.75mV once three bond wires are detached Fig. 10(d)). Figure 11 illustrates the frequency domain output

Authorized licensed use limited to: University of Missouri Libraries. Downloaded on June 03,2023 at 08:53:52 UTC from IEEE Xplore. Restrictions apply.

Table I. Summary of the experimental result for the 50MHz three-sensors test set up using real IGBT.

		Sensor 2		Sensor 3	
Time	Frequency	Healthy	Damaged	Healthy	Damaged
Domain Data		42.4mV	30.4mV	54mV	29.6mV
Frequency Domain Data (FFT)	50MHz	54dB	46dB	57.5dB	55dB
	150MHz	48dB	25dB	No peak	No peak
	200MHz	28.9dB	54dB	No peak	No peak

Table II. Summary of the experimental data for the 20MHz two-sensors test set up using imitation IGBT.

		Sensor 2			
Time Domain Data	Frequency	Initial condition	Single-detached bond wire	Two detached bond wires	Three detached bond wires
		3.6mV	2.3mV	2mV	1.75mV
Frequency Domain Data (FFT)	20MHz	51.5dB	50dB	50dB	49.5dB
	40MHz	31.5dB	27.5dB	No peak	No peak
	80MHz	30dB	30.5dB	No peak	30dB

Table III. Summary of the experimental result for the 20MHz three-sensors test set up using imitation IGBT.

		Sensor 2		Sensor 3	
Time Domain Data	Frequency	Healthy	Damaged	Healthy	Damaged
		1.2 mV	0.4mV	1.6 mV	1.2mV
Frequency Domain Data (FFT)	20MHz	39.75dB	38dB	34dB	32dB
	40MHz	26dB	No peak	26dB	26dB
	60MHz	No peak	No peak	21.5 dB	No peak

corresponding to the time domain data shown in Figure 10. This figure has meaningful information demonstrating differences in fundamental as well as harmonic characteristics during different test conditions.

Figure 12 and Figure 13 show the time and frequency domain data for sensor 2 for the different health status of the imitation IGBT (Test 3: imitation IGBT, 20MHz, three sensors). For instance, the difference between a health condition and a single detached wire bond off V_{P-P} is 0.8mV (Fig. 12). There is also a difference in the frequency domain, 1.5dB (Fig. 13) change has been observed in the primary frequency component. status of the imitation IGBT (Test 3: imitation IGBT, 20MHz, three sensors).

Figure 14 and Figure 15 show the time and frequency domain output of sensor 3 for the different health statuses of the imitation IGBT. The difference in V_{P-P} is .4mV (Fig. 14) for different health states. It has been observed that the frequency domain carries health information as well. These data have been collected for the three sensors system where imitation IGBT has been used. In this experiment, we observed the sensitivity of the three-sensor system using a 20MHz ultrasound oscillator. Table I, Table II, and Table III summarize the entire experimental data.

It is noteworthy that frequency domain data contain no peaks in several cases. It can happen for several reasons such as the distance between the device and sensor, incident angle, frequency, and so on.

IV. Conclusion And Future Work

This manuscript presents a quick, inexpensive and non-destructive technique yet accurate way to detect bond-wire lift-off in conventional high-power IGBT modules. This method does not require any couplant, temperature-dependent complex calculation, or complicated arrangement, and commercially available inexpensive piezoelectric resonators have been used to detect bond-wire detachments inside an IGBT module. Several independent variables such as the number of resonators, resonator frequency, resonator placement, and obviously the number of damaged bond wires collectively determine the time and frequency domain output obtained from the receiver sensor/resonator. This manuscript, therefore, presents the most recent results (as of June 2022) showing that only two resonators can reveal meaningful information about bond-wire-related damages inside an IGBT module.

References

[1] Lai, Wei & Zhao, Yuanpei & Chen, Minyou & Wang, Yueyue & Ding, Xueni & Xu, Shengyou & Pan, Liang-ming. (2018). Condition Monitoring in a Power Module Using On-State Resistance and Case Temperature. IEEE Access. PP. 1-1. 10.1109/ACCESS.2018.2879314.

[2] Shaoyong Yang; Bryant, A.; Mawby, P.; Dawei Xiang; Ran, L.; Tavner, P., "An Industry-Based Survey of Reliability in Power Electronic Converters," Industry Applications, IEEE Transactions on , May-June 2011, vol.47, no.3, pp.1441,1451. [3] S. Dusmez, M. Bhardwaj, L. Sun and B. Akin, "In Situ Condition Monitoring of High-Voltage Discrete Power MOSFET in Boost Converter Through Software Frequency Response Analysis," in IEEE Transactions on Industrial Electronics, vol. 63, no. 12, pp. 7693-7702, Dec. 2016, doi: 10.1109/TIE.2016.2595482.

[3] A. Hanif, A. N. M. Wasekul Azad and F. Khan, "Detection of Bond Wire Lift Off in IGBT Power Modules Using Ultrasound Resonators," 2020 IEEE Applied Power Electronics Conference and Exposition (APEC), 2020, pp. 345-350.

[4] A. Hanif, Y. Yu, D. DeVoto and F. Khan, "A Comprehensive Review Toward the State-of-the-Art in Failure and Lifetime Predictions of Power Electronic Devices," in IEEE Transactions on Power Electronics, May 2019vol. 34, no. 5, pp. 4729-4746.

[5] S. Yang, D. Xiang, A. Bryant, P. Mawby, L. Ran and P. Tavner, "Condition Monitoring for Device Reliability in Power Electronic Converters: A Review," in IEEE Transactions on Power Electronics, Nov. 2010, vol. 25, no. 11, pp. 2734-2752.

[6] S. Roy and F. Khan, "Live condition monitoring of switching devices using SSTDR embedded PWM sequence: A platform for intelligent gate-driver architecture," 2017 IEEE Energy Conversion Congress and Exposition (ECCE), 2017, pp. 3502-3507.

[7] Abu Hanif, Sourov Roy and Faisal Khan, "Detection of gate oxide and channel degradation in SiC power MOSFETs using reflectometry", Wide Bandgap Power Devices and Applications (WiPDA) 2017 IEEE 5th Workshop on, 2017.

[8] A. Hanif, D. DeVoto and F. Khan, "Bond Wire Damage Detection and SOH Estimation of a Dual-Pack IGBT Power Module Using Active Power Cycling and Reflectometry," in IEEE Transactions on Power Electronics, vol. 35, no. 7, pp. 6761-6772, July 2020, doi: 10.1109/TPEL.2019.2958898.

[9] https://muanalysis.com/confocal-scanning-acoustic-microscopy-csam/

[10] S Liu, K Chai, C Zhang, L Jin, Q Yang, "Electromagnetic Acoustic Detection of Steel Plate Defects Based on High-Energy Pulse Excitation", Applied Sciences, 2020 - 10(16), 5534.

[11] Cafarelli, A., Miloro, P., Verbeni, A., Carbone, M., & Menciassi, "A. Speed of sound in rubber-based materialsfor ultrasonic phantoms", Journal of ultrasound, 2016, 19(4), 251-256.

[12] www.nde-ed.org/NDETechniques/Ultrasonics/SelectedApp/weldment

[13] www.nde-d.org/NDETechique/Ultrasonic/Equipment/piezotransducer

Authorized licensed use limited to: University of Missouri Libraries. Downloaded on June 03,2023 at 08:53:52 UTC from IEEE Xplore. Restrictions apply.

Authorized licensed use limited to: University of Missouri Libraries. Downloaded on June 03,2023 at 08:53:52 UTC from IEEE Xplore. Restrictions apply.